PION DISTRIBUTION AMPLITUDE AND PHOTON-TO-PION TRANSITION FORM FACTOR IN QCD*

A.P. Bakulev, S.V. Mikhailov

Bogoliubov Laboratory of Theoretical Physics, JINR, Dubna 141980, Russia
bakulev@theor.jinr.ru

N.G. Stefanis

Institut für Theoretische Physik II, Ruhr-Universität Bochum
44780 Bochum, Germany
stefanis@tp2.ruhr-uni-bochum.de

(Received September 23, 2010)

We discuss the status of the pion distribution amplitude (DA) in connection with QCD sum rules and experimental data on the $\gamma^*\gamma^* \to \pi^0$ transition form factor. Contents: (a) Pion DA in generalized QCD Sum Rules (SRs); (b) Light Cone Sum Rules (LCSR) analysis of the CLEO data for the $\gamma^*\gamma \to \pi^0$ transition form factor; (c) Recent lattice QCD data for the pion DA; (d) BaBar data — a challenge for QCD?

PACS numbers: 12.38.Cy, 14.80.Bn, 12.38.Bx, 11.10.Hi

1. Pion distribution amplitude from QCD sum rules

The *twist-two* pion distribution amplitude (DA) parameterizes the matrix element of the nonlocal axial current on the light cone [1]

$$\langle 0 \,|\, \bar{d}(z)\gamma_\mu\gamma_5[z,0]u(0) \,|\, \pi(P)\rangle\Big|_{z^2=0} = if_\pi P_\mu \int_0^1 dx\; e^{ix(z\cdot P)}\varphi_\pi^{\text{Tw-2}}\left(x,\mu^2\right) . \quad (1)$$

The gauge-invariance of this DA is ensured by the light-like gauge link $[z,0]$, inserted between the two separated quark fields. The physical meaning of this DA is quite evident: it is the amplitude for the transition $\pi(P) \to$

* Presented by A.P. Bakulev at the Workshop "Excited QCD 2010", Tatranská Lomnica/Stará Lesná, Tatra National Park, Slovakia, January 31–February 6, 2010.

$u(Px) + \bar{d}(P(1-x))$. It is convenient to represent the pion DA using an expansion in terms of the Gegenbauer polynomials $C_n^{3/2}(2x-1)$, which are the one-loop eigenfunctions of the ERBL kernel [2, 3]. This representation mean that the whole scale dependence in $\varphi_\pi(x;\mu^2)$ is transformed into the scale dependence of the Gegenbauer-coefficients $a_2(\mu^2), a_4(\mu^2), \ldots$

In order to construct reliable QCD SRs for the pion DA moments, one has to take into account the nonlocality of the QCD vacuum condensates — as it has been shown in [4, 5]. As a concrete example for the nonlocal condensate (NLC) model, we use here the minimal Gaussian model $\langle \bar{q}(0) q(z) \rangle = \langle \bar{q}\, q \rangle\, e^{-|z^2|\lambda_q^2/8}$ with a single scale parameter $\lambda_q^2 = \langle k^2 \rangle$, characterizing the average momentum of quarks in the QCD vacuum. The value of λ_q^2 has been estimated in the QCD SR approach and also on the lattice [6–9]: $\lambda_q^2 = 0.35 - 0.55\,\mathrm{GeV}^2$.

The NLC SRs for the (twist-2) pion DA produce a bunch of self-consistent two-parameter models at the normalization scale $\mu_0^2 \simeq 1.35\,\mathrm{GeV}^2$:

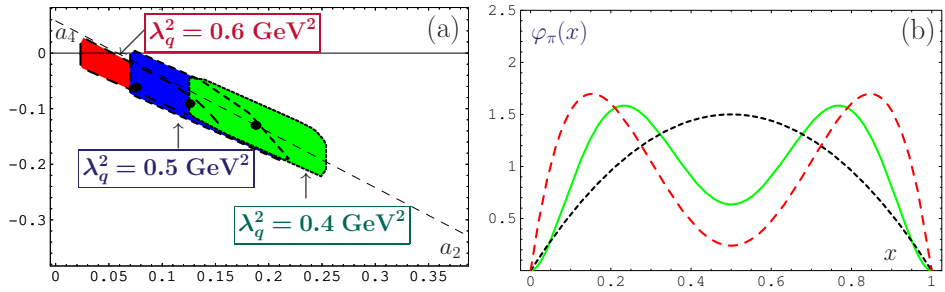

Fig. 1. (a): The allowed values of the parameters a_2 and a_4 of the pion DA bunch (2), evaluated at $\mu^2 = 1.35\,\mathrm{GeV}^2$ for three values of the nonlocality parameter $\lambda_q^2 = 0.4, 0.5$, and $0.6\,\mathrm{GeV}^2$. (b): Shapes of three characteristic pion DAs — BMS (solid line), CZ (dashed line), and the asymptotic DA (dotted line).

$$\varphi_\pi^{\mathrm{NLC}}(x;\mu_0^2) = \varphi^{\mathrm{As}}(x)\Big[1 + a_2(\mu_0^2)\, C_2^{3/2}(2x-1) + a_4(\mu_0^2)\, C_4^{3/2}(2x-1)\Big]\,. \quad (2)$$

The central point corresponds to $a_2^{\mathrm{BMS}} = +0.188$, $a_4^{\mathrm{BMS}} = -0.130$ for $\lambda_q^2 = 0.4\,\mathrm{GeV}^2$, whereas other allowed values of the parameters a_2 and a_4 — in correspondence with associated values of λ_q^2 — are shown in the left panel of Fig. 1 in the form of slanted rectangles [10]. All these solutions yield, in accord with (2), the same value of the inverse moment of the pion DA, namely, $\langle x^{-1} \rangle_\pi^{\mathrm{bunch}} = 3.17 \pm 0.20$. This range is in a good agreement with the estimates derived from a dedicated SR for this moment which can be obtained through the basic SR by integrating over x with the corresponding

weight x^{-1} (at $\mu_0^2 \simeq 1.35\,\mathrm{GeV}^2$): $\langle x^{-1}\rangle_\pi^{\mathrm{SR}} = 3.30 \pm 0.30$. It is worth emphasizing at this point that the moment $\langle x^{-1}\rangle_\pi^{\mathrm{SR}}$ can be safely determined only with the use of NLC SRs because of the absence of endpoint singularities.

Comparing the obtained pion DA with the Chernyak–Zhitnitsky (CZ) one [11], reveals that, although both DAs are two-humped, they are quite different, with the BMS DA being strongly endpoint suppressed (see Fig. 1(a)).

Qualitatively similar results have also been obtained with the improved Gaussian model of the nonlocal QCD vacuum [12]. In that case, the allowed region for the parameters a_2 and a_4 in Fig. 1(a) is shifted along the diagonal farther to the right with the central point being located near the right corner of the allowed, light grey (green) region. We emphasize that the BMS model [10] is inside the allowed region obtained with the improved QCD vacuum model. This means that the characteristic features of the BMS bunch persist for the improved bunch as well — in particular the endpoint suppression.

2. Analysis of the CLEO data on $F_{\gamma\gamma^*\pi}(Q^2)$ and the pion DA

Many studies [9, 15, 21–25] have been performed to determine the pion DA characteristics using the high-precision CLEO data [14] on the pion–photon transition form factor $F_{\pi\gamma^*\gamma}(Q^2)$. For instance, we have used in [15] LCSRs [21, 26] with next-to-leading-order accuracy of QCD perturbation theory with the aim to analyze the theoretical uncertainties involved in the CLEO-data analysis and extract more reliable estimates for the first two coefficients a_2 and a_4, which parameterize the deviation from the asymptotic expression $\varphi_\pi^{\mathrm{As}}$. The upshot of our analysis [15, 27] is that the CZ DA is excluded at the 4σ-level, whereas the asymptotic DA is off at the 3σ-level, while the BMS DA (and most of the BMS bunch) is inside the 1σ-error ellipse, and the instanton-based model of Ref. [28] is close to the 2σ-boundary. Moreover, we found that the CLEO data conform with the value of the QCD nonlocality parameter $\lambda_q^2 = 0.4\ \mathrm{GeV}^2$.

3. Pion form factor and JLab data

In this context it is worth mentioning our analysis of the pion's electromagnetic form factor which employs NLC QCD SRs, Analytic QCD Perturbation Theory, and NLC-derived pion DAs [16]. The obtained results are in excellent agreement with the recent JLab data and also with the lattice data of Ref. [17], as one sees from Fig. 2(b), where the light gray strip includes the NLC QCD SRs uncertainties, whereas the dark gray strip represents the lattice results.

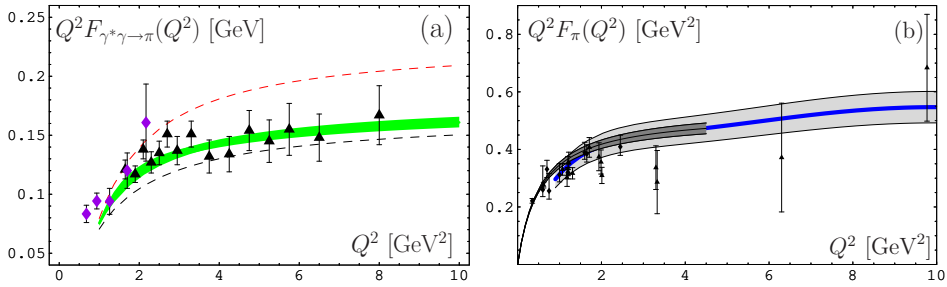

Fig. 2. (a): LCSR predictions for $Q^2 F_{\gamma^*\gamma\to\pi}(Q^2)$ for the CZ DA (upper dashed line), BMS-bunch (shaded strip), and the asymptotic DA (lower dashed line) in comparison with the CELLO (diamonds, [13]) and the CLEO (triangles, [14]) experimental data, evaluated with the twist-4 parameter value $\delta^2_{\text{tw}-4} = 0.19\,\text{GeV}^2$ [15] and at $\mu^2_{\text{SY}} = 5.76\,\text{GeV}^2$. (b): The scaled pion form factor calculated in the NLC QCD SRs, solid (blue) line, including nonperturbative uncertainties (shaded strip) [16]. The dark gray strip shows the lattice data [17] and the experimental data are taken from [18] (diamonds) and [19, 20] (triangles).

4. New lattice data and the pion DA

Rather recently, new high-precision lattice measurements of the second moment of the pion's DA $\langle\xi^2\rangle_\pi = \int_0^1 (2x-1)^2 \varphi_\pi(x)\,dx$ appeared [30, 31]. Both groups extracted from their respective simulations, values of a_2 at the Schmedding–Yakovlev scale $\mu^2_{\text{SY}} \approx 0.24$, but with different error bars. Remarkably, these lattice results are in striking agreement with the estimates for a_2 both from NLC QCD SRs [10] and also from the CLEO-data analyses based on LCSRs [15, 21]. The improved bunch [12] appears to have an even better agreement with the recent lattice results [31].

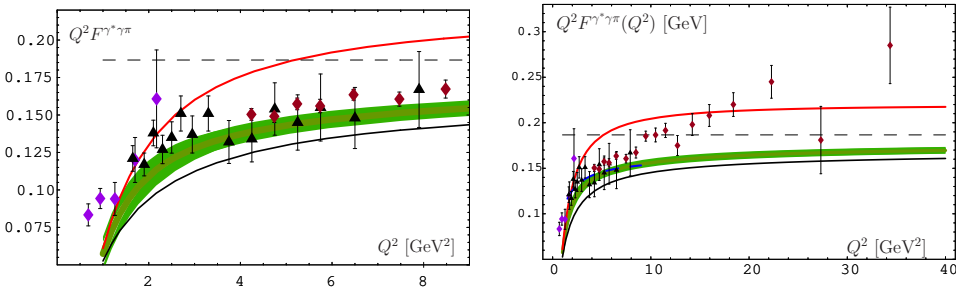

Fig. 3. NNLO$_{\beta_0}$ LCSR predictions for $Q^2 F_{\gamma^*\gamma\to\pi}(Q^2)$ for the CZ DA, upper (red) line, BMS-bunch (shaded green strip), and the asymptotic DA (lower solid line) in comparison with the CELLO, CLEO (the same as in Fig. 1(a)) and BaBar [29] diamonds (brown) with much smaller error-bars experimental data. Left panel: $Q^2 \le 9\,\text{GeV}^2$ region. Right panel: whole BaBar region of Q^2.

5. Confronting NNLO LCSR results for $F_{\gamma^*\gamma\to\pi}$ with the BaBar data

In a recent paper by two of us [32], the NNLO QCD radiative corrections, proportional to the β_0-coefficient, have been calculated and included into the LCSR analysis of the pion–photon transition form factor. The overall effect of these corrections appears to be negative, hence reducing the $\gamma^*\gamma \to \pi^0$ form factor by -7% at low $Q^2 \sim 2\,\text{GeV}^2$ and by -2.5% at intermediate $Q^2 \gtrsim 6\,\text{GeV}^2$ (left panel in Fig. 3). In spite of this reduction, the BMS bunch describes rather well all data for $Q^2 \in [1.5, 9]$ GeV^2 — including those of BaBar [29]. This means that the CLEO (and the low-energy BaBar) data are incompatible with wide pion DAs and demand that the endpoints $x = 0, 1$ are stronger suppressed than in the asymptotic DA.

Surprisingly, the BaBar data [29] contradict this behavior in the high-energy region: there, they show a significant growth with Q^2 for values above $\sim 10\,\text{GeV}^2$. This behavior of the BaBar data is clearly in conflict with the collinear factorization in perturbative QCD. This is true for any pion DA that vanishes at the endpoints $x = 0, 1$ (see Fig. 3 — right panel) and the explanations in [32].

Despite the appearance of several proposals to explain the anomalous behavior of the high-Q^2 BaBar data [33–36], we want to emphasize that from the point of view of QCD it is not possible to describe them either with the inclusion of higher radiative corrections or with higher-twists — both types of contributions are negative [15, 32, 37].

6. Conclusions

To conclude, the QCD SRs produce an endpoint-suppressed bunch of pion DAs in agreement with the CELLO and the CLEO data on $F_{\gamma^*\gamma\to\pi}$. The second moment of these DAs is within the range found in recent lattice simulations. These results are also in line with the new BaBar data up to $\sim 10\,\text{GeV}^2$ but do not reproduce the observed growth above this scale. It was shown in [38] that the CELLO and the CLEO data cannot be fitted simultaneously with all the BaBar data.

This investigation was supported in part by the Heisenberg–Landau Program, Grant 2010, and the Russian Foundation for Fundamental Research, Grants No. 07-02-91557, 08-01-00686 and 09-02-01149.

REFERENCES

[1] A.V. Radyushkin, Dubna preprint P2-10717, 1977 [hep-ph/0410276].
[2] A.V. Efremov, A.V. Radyushkin, *Phys. Lett.* **B94**, 245 (1980).
[3] G.P. Lepage, S.J. Brodsky, *Phys. Lett.* **B87**, 359 (1979).
[4] S.V. Mikhailov, A.V. Radyushkin, *JETP Lett.* **43**, 712 (1986).
[5] A.P. Bakulev, S.V. Mikhailov, *Phys. Lett.* **B436**, 351 (1998).
[6] V.M. Belyaev, B.L. Ioffe, *Sov. Phys. JETP* **56**, 493 (1982).
[7] A.A. Ovchinnikov, A.A. Pivovarov, *Sov. J. Nucl. Phys.* **48**, 721 (1988).
[8] M. D'Elia, A. Di Giacomo, E. Meggiolaro, *Phys. Rev.* **D59**, 054503 (1999).
[9] A.P. Bakulev, S.V. Mikhailov, *Phys. Rev.* **D65**, 114511 (2002).
[10] A.P. Bakulev, S.V. Mikhailov, N.G. Stefanis, *Phys. Lett.* **B508**, 279 (2001); [Erratum *Phys. Lett.* **B590**, 309 (2004)].
[11] V.L. Chernyak, A.R. Zhitnitsky, *Nucl. Phys.* **B201**, 492 (1982).
[12] A.P. Bakulev, A.V. Pimikov, *Phys. Part. Nucl. Lett.* **4**, 377 (2007); *Acta Phys. Pol. B* **37**, 3627 (2006).
[13] H.J. Behrend *et al., Z. Phys.* **C49**, 401 (1991).
[14] J. Gronberg *et al., Phys. Rev.* **D57**, 33 (1998).
[15] A.P. Bakulev, S.V. Mikhailov, N.G. Stefanis, *Phys. Rev.* **D67**, 074012 (2003).
[16] A.P. Bakulev, A.V. Pimikov, N.G. Stefanis, *Phys. Rev.* **D79**, 093010 (2009).
[17] D. Brommel *et al., Eur. Phys. J.* **C51**, 335 (2007).
[18] J. Volmer *et al., Phys. Rev. Lett.* **86**, 1713 (2001).
[19] C.N. Brown *et al., Phys. Rev.* **D8**, 92 (1973).
[20] C.J. Bebek *et al., Phys. Rev.* **D13**, 25 (1976).
[21] A. Schmedding, O. Yakovlev, *Phys. Rev.* **D62**, 116002 (2000).
[22] N.G. Stefanis, W. Schroers, H.-C. Kim, *Phys. Lett.* **B449**, 299 (1999).
[23] N.G. Stefanis, W. Schroers, H.-C. Kim, *Eur. Phys. J.* **C18**, 137 (2000).
[24] E. Ruiz Arriola, W. Broniowski, *Phys. Rev.* **D66**, 094016 (2002).
[25] S.S. Agaev, *Phys. Rev.* **D72**, 074020 (2005).
[26] A. Khodjamirian, *Eur. Phys. J.* **C6**, 477 (1999).
[27] A.P. Bakulev, S.V. Mikhailov, N.G. Stefanis, *Phys. Lett.* **B578**, 91 (2004).
[28] M. Praszałowicz, A. Rostworowski, *Phys. Rev.* **D64**, 074003 (2001).
[29] B. Aubert *et al.*, *Phys. Rev.* **D80**, 052002 (2009).
[30] L. Del Debbio, *Few Body Syst.* **36**, 77 (2005).
[31] V.M. Braun *et al.*, *Phys. Rev.* **D74**, 074501 (2006).
[32] S.V. Mikhailov, N.G. Stefanis, *Nucl. Phys.* **B821**, 291 (2009).
[33] A.E. Dorokhov, arXiv:0905.4577[hep-ph].
[34] A.V. Radyushkin, *Phys. Rev.* **D80**, 094009 (2009).
[35] M.V. Polyakov, *JETP Lett.* **90**, 228 (2009).
[36] V.L. Chernyak, arXiv:0912.0623[hep-ph].
[37] A.P. Bakulev, S.V. Mikhailov, N.G. Stefanis, *Phys. Rev.* **D73**, 056002 (2006).
[38] S.V. Mikhailov, N.G. Stefanis, *Mod. Phys. Lett.* **A24**, 2858 (2009).